Route Generation for Drone Delivery Service Using an Evolutionary Multi-Objective Optimization Method

OMAGARI, Hiroki
Department of Aeronautics and Astronautics, Kyushu University

Higashino, Shin-Ichiro
Department of Aeronautics and Astronautics, Kyushu University

出版情報：Transactions of the Japan Society for Aeronautical and Space Sciences, Aerospace Technology Japan. 18 (4), pp.123-132, 2020. 日本航空宇宙学会
バージョン：

Trans. JSASS Aerospace Tech. Japan
Vol. 18, No. 4, pp. 123-132, 2020
DOI: 10.2322/tastj.18.123

Route Generation for Drone Delivery Service Using an Evolutionary Multi-Objective Optimization Method

By Hiroki OMAGARI[1)] and Shin-Ichiro HIGASHINO[1)]

[1)] *Department of Aeronautics and Astronautics, Kyushu University, Fukuoka, Japan*

(Received November 13th, 2019)

The purpose of our research is to formulate a drone delivery problem (DDP) as a constrained multi-objective optimization problem and evaluate the cost-reduction effect of a drone delivery service using the provisional-ideal-point (PIP) method proposed in this paper. The original PIP method is a genetic algorithm-based (GA-based) optimization method that can efficiently generate a preferred solution for a decision-maker. However, there are two problems occur when this method is applied to the DDP. The first problem is that there exist some cases wherein the evaluation function becomes infinite in the search process, making it impossible to sort the generated solutions. The second problem is that a long time is needed for the solution search to converge. Accordingly, the process had to be aborted at the halfway point. We present an improved PIP method to overcome these two problems. The proposed method is a solution search comprising a GA combined with tabu search. It converts the DDP into a single-objective optimization problem of a delivery cost using conversion factors. This paper presents several things understood regarding the cost-reduction effect on drone delivery services using our newly proposed method.

Key Words: Drone Delivery Service, Multi-Objective Optimization, Genetic Algorithm, Tabu Search, Conversion Factor

Nomenclature

A	:	number of available trucks
B	:	number of available drones per truck
CF_I	:	conversion factor of $F_I(x)$
C_{ideal}	:	position vector of provisional ideal point
C_{sol}	:	position vector of solution point
C_{total}	:	total delivery cost
DC	:	flight distance cost between WPs, m
D_{is}	:	distance between C_{ideal} and C_{sol}
D^j, D^{ij}	:	drone delivery route
E_n	:	elite number
$F(x)$	:	objective function
$F_{I_{pro}}$	:	provisional optimal value of $F_I(x)$
$g_J(x)$	:	J-th constrained condition
g, g'	:	generations
G_{max}	:	maximum generations in solution search
G_{tabu}	:	maximum generations in tabu search
$h_{a,ij}$	:	number of WP in D_a^{ij}
L_d	:	position of depot
LD_{max}	:	maximum travel distance, m
LT_{max}	:	maximum delivery time, s
m	:	total number of constrained conditions
M	:	total number of objective functions
ND_j	:	total number of WP visited by j-th drone
NH_i	:	total number of WP visited by i-th truck
NT_i	:	total number of WP visited by i-th truck
N_{WP}	:	total number of WP
p, p'	:	set of solutions
P_n	:	population
$P(x)$	:	penalty function
R	:	relative drone-to-truck cost ratio
s	:	number of solutions in p or p'
T	:	tabu lists
TC	:	distance cost between WPs, m
T^i	:	truck delivery route
t_d	:	flight duration time of drone, s
t_p	:	parking time at WP, s
t_{re}	:	battery replacement time, s
t_{tl}	:	take-off or landing time of drone, s
T^i	:	truck delivery route for i-th truck
u^{ij}	:	set of u_a^{ij}
V_D	:	flight velocity of drone, m/s
V_T	:	travel velocity of truck, m/s
$w_{a,b}^{ij}$	:	package weight, kg
W_d	:	loadable weight of drone, kg
WP	:	depot or delivery position
x, x', x''	:	generated solution
x^*	:	best solution in p
x_{best}	:	preferred solution
x_F	:	feasible solution

1. Introduction

In recent years, the use of drones has become widespread not only in the military field, but also in a variety of applications such as infrastructure inspection,[1] monitoring,[2] pesticide spraying,[3] aerial photography,[4] transport of relief supplies,[5] and hobbies[6] because of their ease of operation and low cost. Drone delivery service also became a hot topic in 2013 with the announcement of "Amazon Prime Air."[7] Since then, several venture companies and organizations around the world have been attempting to introduce drone delivery services.

This service is also expected to be quite effective in Japan because a shortage of drivers has become a serious social problem.[8] It can also be used to deliver relief supplies to affected areas when a disaster occurs.

The applications suitable for drone delivery are, however, limited owing to the limitations in flight duration, loadable weight, and robustness to wind. One of the methods used to compensate for the weakness of the drones is called "last-mile deliveries" or "last-mile distribution."[9, 10] In this method, drones are only used for delivering the packages to destinations over a short distance, while the majority of the delivery distance is covered using trucks. Murray et al. quantitatively evaluated how much last-mile deliveries can reduce the travel distance and time as compared to those of truck delivery.[11-14] Chiang et al. also presented the benefits of last-mile deliveries in terms of reducing CO_2 emissions as well as delivery costs.[15, 16]

In this paper, we refer to the delivery service comprising only the use of trucks as "truck delivery," that comprising only the use of drones as "drone delivery," and the service combining the use trucks and drones as "hybrid delivery." Figures 1(a) through 1(c) are conceptual diagrams of these delivery styles.

A route-generation problem related to the drone delivery and the hybrid delivery is referred to as a "drone delivery problem (DDP)." A DDP can be formulated as a constrained multi-objective optimization problem. In our past studies, we presented a multi-objective optimization method called the "provisional-ideal-point (PIP) method," which is based on using a genetic algorithm (GA) for solving the DDP.[13] However, two problems occur when this method is applied to the DDP. The first problem is that there exist some cases wherein the evaluation function value of the original PIP method is infinite because the evaluation function characteristics make it impossible to sort the generated solutions. We refer to this problem as the "division by zero (DBZ) problem." The second problem is that it is difficult to use "crossover" operators for the DDP because solution structures such as the hybrid delivery routes are complicated. Therefore, when applying the original PIP method to the DDP, it is necessary to depend only on "mutation" operators. However, this kind of method often terminates the calculation in the middle of the solution search because it takes a long time to converge. We refer to this problem as the "immature convergence (IC) problem."

In this paper, we present two methods for solving these two problems. The first method involves unifying the objective functions of the DDP to a delivery cost using conversion factors. The conversion factors provide correlations between the objective functions and make it possible to prevent the occurrence of the DBZ problem. The second method is to use "tabu search (TS)" for solving the IC problem. TS enables a global solution search by intentionally abandoning the best solution in the population to prevent stagnating the solution search.[17] Combining this method with the original PIP method can be expected to improve the efficiency of the solution search.

The usefulness of the improved PIP method can be verified via some benchmark problems from the "traveling salesman problem library (TSPLIB)."[18] The validity of this method can also be demonstrated by applying it to the DDP.

In addition, the cost-reduction effects of the drone delivery and the hybrid delivery as compared to the truck delivery are evaluated using the improved PIP method. From these calculation results, much knowledges regarding the cost-reduction effect of the drone delivery service can be obtained.

This paper is structured as follows. Section 2 describes the original and the improved PIP methods. Section 3 describes the solution structure of the DDP and its mutation operators. Section 4 presents the formulation of the DDP as a constrained multi-objective optimization problem, the calculation method for conversion factors, and problem settings of the DDP. Section 5 presents an investigation of the usefulness of the improved PIP method using some kinds of the TSPLIB and the DDP. In addition, the relationship between the cost-reduction effect and relative cost ratio of the drone to the truck is analyzed. Several obtained knowledges regarding the cost-reduction effect of drone delivery service are then presented. Section 6 presents the conclusions of this study.

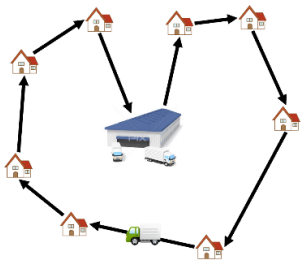

Fig. 1(a). Truck delivery.

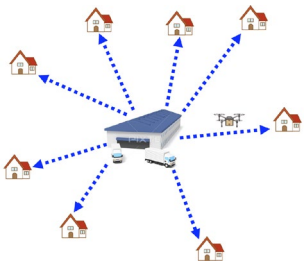

Fig. 1(b). Drone delivery.

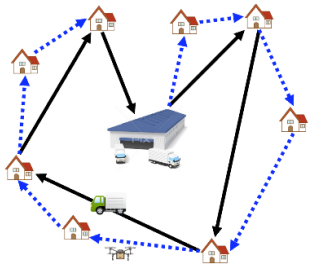

Fig. 1(c). Hybrid delivery.

2. PIP Method

The DDP can be formulated as a constrained multi-objective optimization problem as shown in Eq. (1).

$$\begin{cases} \min\limits_{\boldsymbol{x}} \boldsymbol{F}(\boldsymbol{x}) = \min\limits_{\boldsymbol{x}} [F_1(\boldsymbol{x}), F_2(\boldsymbol{x}), \ldots, F_I(\boldsymbol{x}), \ldots, F_M(\boldsymbol{x})]^T \\ subject\ to\ F_I(\boldsymbol{x}) \geq 0\ (I = 1,2,\ldots,M), \\ \qquad\qquad g_J(\boldsymbol{x}) \leq 0\ (J = 1,2,\ldots,m) \end{cases} \tag{1}$$

It should be noted that optimization means minimization in

this paper. We assume that $F_I(\boldsymbol{x})$ in the DDP is positive. However, if $F_I(\boldsymbol{x})$ is negative, $F_I(\boldsymbol{x})$ should be transformed to $F_I(\boldsymbol{x}) \geq 0$ by an appropriate means so that the magnitude relation of $F_I(\boldsymbol{x})$ does not change.

2.1. Original PIP method

The original PIP method performs a solution search using the two procedures presented below.[13)]

<*Procedure 1*> (Search for feasible solutions)

The penalty function $P(\boldsymbol{x})$ is defined as shown in Eq. (2).

$$P(\boldsymbol{x}) = \sum_{J=1}^{m} P_J(\boldsymbol{x}) \quad s.t. \begin{cases} P_J(\boldsymbol{x}) = g_J(\boldsymbol{x}), & g_J(\boldsymbol{x}) > 0 \\ P_J(\boldsymbol{x}) = 0, & g_J(\boldsymbol{x}) \leq 0 \end{cases} \tag{2}$$

$\boldsymbol{x_F}$ can be generated by searching for $\boldsymbol{x}$, which satisfies $P(\boldsymbol{x}) = 0$. As a unique feature of this method, the units of $g_J(\boldsymbol{x})$ are ignored, and they are added as scalar values. Such a calculation is allowed because the generation of $\boldsymbol{x_F}$ is the objective of the solution search. The first procedure is complete when $\boldsymbol{x_F}$ is generated.

<*Procedure 2*> (Multi-objective optimization)

$F_{I_{pro}}$ is defined for each objective function. $F_{I_{pro}}$ represents the smallest value of $F_I(\boldsymbol{x_F})$ obtained using the solution search up to the current generation. $F_{I_{pro}}$ is updated every time a better solution is found. Using this value, two types of coordinates are defined: the "solution point $\boldsymbol{C_{sol}}(\boldsymbol{x_F})$" and "provisional ideal point $\boldsymbol{C_{ideal}}$," as shown in Eqs. (3) and (4), respectively.

$$\boldsymbol{C_{sol}}(\boldsymbol{x_F}) = \left[\frac{F_1(\boldsymbol{x_F})}{F_{1_{pro}}}, \ldots, \frac{F_I(\boldsymbol{x_F})}{F_{I_{pro}}}, \ldots, \frac{F_M(\boldsymbol{x_F})}{F_{M_{pro}}}\right]^T \tag{3}$$

$$\boldsymbol{C_{ideal}} = \left[\frac{F_{1_{pro}}}{F_{1_{pro}}}, \ldots, \frac{F_{I_{pro}}}{F_{I_{pro}}}, \ldots, \frac{F_{M_{pro}}}{F_{M_{pro}}}\right]^T = [1, \ldots, 1, \ldots, 1]^T \tag{4}$$

$\boldsymbol{C_{sol}}(\boldsymbol{x_F})$ is a coordinate of $\boldsymbol{x_F}$. $\boldsymbol{C_{ideal}}$ is the coordinate of a virtual solution where all of the objective functions are simultaneously optimized to $F_{I_{pro}}$. The original PIP method can search for a preferred solution for a decision-maker by minimizing $D_{is}(\boldsymbol{x_F})$, as shown in Eq. (5).

$$\begin{cases} \min\limits_{\boldsymbol{x}} \boldsymbol{F}(\boldsymbol{x}) = \min\limits_{\boldsymbol{x}} D_{is}(\boldsymbol{x_F}) = \min\limits_{\boldsymbol{x}} \|\boldsymbol{C_{ideal}} - \boldsymbol{C_{sol}}(\boldsymbol{x_F})\| \\ \qquad = \min\limits_{x} \left(\sum\limits_{I=1}^{M} \left(1 - \dfrac{F_I(\boldsymbol{x_F})}{F_{I_{pro}}}\right)^2 \right)^{\frac{1}{2}} \\ subject\ to\ P(\boldsymbol{x}) = 0 \end{cases} \tag{5}$$

2.2. Improved PIP method

2.2.1. Conversion factors

If $F_{I_{pro}} = 0$, $F_I(\boldsymbol{x_F})/F_{I_{pro}}$ becomes a division-by-zero calculation, which is the DBZ problem. We propose the introduction of conversion factors that unify all of the objective functions into specific units to solve the DBZ problem. All of the objective functions can be converted into a delivery cost in the DDP. In this case, Eqs. (3) and (4) are redefined as Eqs. (6) and (7).

$$\boldsymbol{C_{sol}}(\boldsymbol{x_F}) = [CF_1 \times F_1(\boldsymbol{x_F}), \ldots, CF_M \times F_M(\boldsymbol{x_F})]^T \tag{6}$$

$$\boldsymbol{C_{ideal}} = \left[CF_1 \times F_{1_{pro}}, \ldots, CF_M \times F_{M_{pro}}\right]^T \tag{7}$$

CF_I is uniquely calculated using actual information related to the delivery service. With respect to the delivery cost, correlations between the objective functions can be obtained by substituting Eqs. (6) and (7) into Eq. (5). As a result, $D_{is}(\boldsymbol{x_F})$ is not infinite, and occurrence of the DBZ problem can be prevented.

In addition, the total delivery cost is calculated by summing all of the terms in Eq. (6), as shown in Eq. (8).

$$C_{total}(\boldsymbol{x_F}) = \sum_{I=1}^{M} \left(CF_I \times F_I(\boldsymbol{x_F})\right) \tag{8}$$

2.2.2. Tabu search (TS)

The application method for TS in the improved PIP method is shown below.

In Procedure 1, the state where the value of $P(\boldsymbol{x})$ is not updated over G_{tabu} generation is regarded as stagnation of the solution search and excludes the best solution from the population. At this time, the best solution to be excluded is recorded in a tabu list (TL). In the subsequent solution search, the generated solutions will also be excluded if they are the same as the solution recorded in the TL. In doing so, the solution search does not stagnate with the same solution and a more global solution search can be performed.

In Procedure 2, the same operation as Procedure 1 is performed for $D_{is}(\boldsymbol{x_F})$, not $P(\boldsymbol{x})$. When the number of generations reaches G_{max}, the solution with the smallest $C_{total}(\boldsymbol{x_F})$ in the TL is selected as the preferred solution.

The following procedures are the above solution search process organized in each step.

<*Procedure 1*> (Search for feasible solutions)

<*Step 1*>
$g \leftarrow 0$ and $g' \leftarrow 0$.
<*Step 2*>
A set p including s initial individuals $\boldsymbol{x}$ is generated. Then, $g \leftarrow g + 1$.
<*Step 3*>
$\boldsymbol{x}'$, where $P(\boldsymbol{x}') \leq P(\boldsymbol{x})$ $(\boldsymbol{x}' \in p, \forall \boldsymbol{x} \in p)$, is defined as $\boldsymbol{x}^* \leftarrow \boldsymbol{x}'$.
<*Step 4*>
If $P(\boldsymbol{x}^*) = 0$, proceed to <***Procedure 2***> with $\boldsymbol{x_F}^* \leftarrow \boldsymbol{x}^*$.
<*Step 5*>
A set composed of $\boldsymbol{x}^*$ and $s-1$ individuals $\boldsymbol{x}$ generated by the mutation of $\boldsymbol{x}^*$ is defined as p'. Then, $p \leftarrow p'$ and $g \leftarrow g + 1$.
<*Step 6*>
If $g > G_{max}$, proceed to <*Step 11*>.
<*Step 7*>
$\boldsymbol{x}$ included in TL is eliminated from p.
<*Step 8*>
If $g' \leq G_{tabu}$, return to <*Step 3*>.
<*Step 9*>
If $g' > G_{tabu}$, $\boldsymbol{x}^*$ is added into TL.
<*Step 10*>
$\boldsymbol{x}$ is selected other than $\boldsymbol{x}^*$ from p arbitrary and $\boldsymbol{x}^* \leftarrow \boldsymbol{x}$. Then, return to <*Step 5*> with $g' \leftarrow 0$.
<*Step 11*>
Regard **<*Procedure 1*>** as a failure and reconsider the problem settings.

<*Procedure 2*> (Multi-objective optimization)

<*Step 12*>

TL is initialized as an empty cell array and $g' \leftarrow 0$.
<*Step 13*>
A set composed of $\boldsymbol{x_F}^*$ and $s-1$ individuals $\boldsymbol{x}$ generated by the mutation of $\boldsymbol{x_F}^*$ is defined as p'. Then, $p \leftarrow p'$ and $g \leftarrow g+1$.
<*Step 14*>
$\boldsymbol{x_F}'$ is selected, where $F_l(\boldsymbol{x_F}') \leq F_l(\boldsymbol{x_F})$ $(\boldsymbol{x_F}' \in p, \forall \boldsymbol{x_F} \in p, l = 1,2,\dots,M)$ and $F_{l_{pro}} \leftarrow F_l(\boldsymbol{x_F}')$.
<*Step 15*>
$\boldsymbol{x_F}''$ is selected, where $D_{is}(\boldsymbol{x_F}'') \leq D_{is}(\boldsymbol{x})$ $(\boldsymbol{x_F}'' \in p, \forall \boldsymbol{x_F} \in p)$ and $\boldsymbol{x_F}^* \leftarrow \boldsymbol{x_F}''$.
<*Step 16*>
If $g > G_{max}$, proceed to <*Step 21*>.
<*Step 17*>
$\boldsymbol{x_F}$ included in TL is eliminated from p.
<*Step 18*>
If $g' \leq G_{tabu}$, return to <*Step 13*>.
<*Step 19*>
If $g' > G_{tabu}$, $\boldsymbol{x_F}^*$ is added into TL.
<*Step 20*>
$\boldsymbol{x_F}$ is selected other than $\boldsymbol{x_F}^*$ from p arbitrary and $\boldsymbol{x_F}^* \leftarrow \boldsymbol{x_F}$. If there is no $\boldsymbol{x_F}$ except for $\boldsymbol{x_F}^*$ in p, remove $\boldsymbol{x_F}^*$ from TL and return to <*Step 13*>. Otherwise, return to <*Step 13*> with $g' \leftarrow 0$.
<*Step 21*>
$\boldsymbol{x_{best}}$ is selected, where $C_{total}(\boldsymbol{x_{best}}) \leq C_{total}(\boldsymbol{x_F})$ $(\boldsymbol{x_{best}} \in TL, \forall \boldsymbol{x_F} \in TL)$ as the preferred solution.

3. Genetic Algorithm

The solution structures expressing three types of delivery-route styles are shown in Figs. 1(a) through 1(c), and their mutation operators are presented below.

3.1. Truck delivery route

Equation (9) represents the solution structure of the truck delivery route.

$$T^i = [L_d, T_1^i, T_2^i, \dots, T_a^i, \dots, T_{NT_i}^i, L_d] \quad (i = 1,2,\dots,A \;\; a = 1,2,\dots,NT_i) \tag{9}$$

Figure 2 shows a conceptual diagram of T^i.

Fig. 2. Conceptual diagram of T^i.

T^i represents a traveling route that starts from a depot, and WPs delivered by a truck are arranged in the order of delivery. T_a^i is assigned one of the WPs. Three types of mutation operators for T^i are presented below. It should be noted that $a1$, $a2$, $l1$, and $l2$ are arbitrary integers in the domain presented in Eqs. (10) and (11).

$$1 \leq a1 \leq a2 \leq A \tag{10}$$
$$1 \leq l1 \leq l2 \leq NT_i \tag{11}$$

Operator 1 :
A part of T^{a1} from T_{l1}^{a1} to T_{l2}^{a1} is inserted into an arbitrary place between two WPs of T^{a2}.
Operator 2 :
A part of T^{a1} from T_{l1}^{a1} to T_{l2}^{a2} is reversed.
Operator 3 :
T_{l1}^{a1} is selected from T^{a1} and T_{l2}^{a2} is selected from T^{a2}. They are then swapped with each other.

3.2. Drone delivery route

Equation (12) represents the solution structure of the drone delivery route.

$$D^j = [D_1^j, D_2^j, \dots, D_b^j, \dots, D_{ND_j}^j] \quad (j = 1,2,\dots,B \;\; b = 1,2,\dots,ND_j) \tag{12}$$

Figure 3 shows a conceptual diagram of D^j.

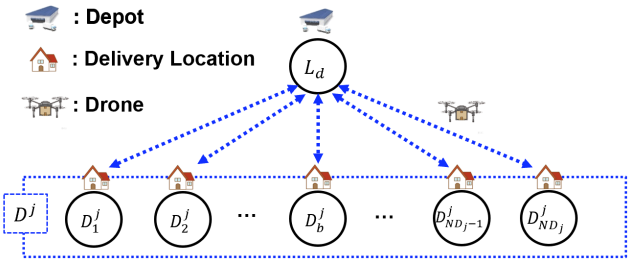

Fig. 3. Conceptual diagram of D^j.

D^j represents the flight delivery routes between a depot and each WP, and the WP delivered by a drone is arranged in the order of delivery. D_b^j is one of the WPs. Two types of mutation operators for D^j are presented below. It should be noted that $b1$, $b2$, $m1$, and $m2$ are arbitrary integers in the domain presented in Eqs. (13) and (14).

$$1 \leq b1 \leq b2 \leq B \tag{13}$$
$$1 \leq m1 \leq m2 \leq ND_j \tag{14}$$

Operator 4 :
D_{m1}^{b1} is selected from D^{b1} and inserted into an arbitrary place of D^{b2}.
Operator 5 :
D_{m1}^{b1} is selected from D^{b1} and D_{m2}^{b2} is selected from D^{b2}. They are then swapped with each other.

3.3. Hybrid delivery route

Equations (15) through (17) represent the solution structure of the hybrid delivery route.

$$T^i = [L_d, T_1^i, T_2^i, \dots, T_a^i, \dots, T_{NH_i}^i, L_d] \quad (a = 1,2,\dots,NH_i) \tag{15}$$
$$D^{ij} = [D_{L_d}^{ij}, D_1^{ij}, D_2^{ij}, \dots, D_a^{ij}, \dots, D_{NH_i}^{ij}] \tag{16}$$
$$u^{ij} = [u_{L_d}^{ij}, u_1^{ij}, u_2^{ij}, \dots, u_a^{ij}, \dots, u_{NH_i}^{ij}] \quad u_a^{ij} \in \{0,1\} \tag{17}$$

Figure 4 presents a conceptual diagram of T^i, D^{ij}, and u^{ij}.

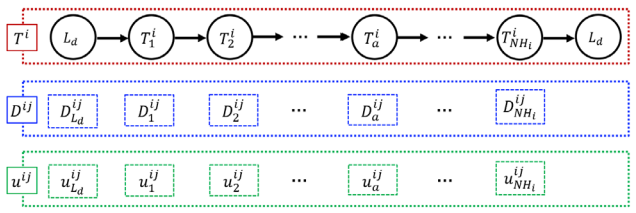

Fig. 4. Conceptual diagram of T^i, D^{ij} and u^{ij}.

The hybrid delivery route is obtained by combining the three solution structures of T^i, D^{ij}, and u^{ij}. T^i represents the traveling route of a truck starting from a depot, and the WPs delivered by the truck are arranged in the order of delivery. D^{ij} is a set of D_a^{ij}, and D_a^{ij} is a set of WPs delivered by the drone,

which takes off at T_a^i as shown in Eq. (18).

$$D_a^{ij} = \left[D_{a,1}^{ij}, D_{a,2}^{ij}, \ldots, D_{a,b}^{ij}, \ldots, D_{a,h_{a,ij}}^{ij}\right] \quad (b = 1,2,\ldots,h_{a,ij}) \tag{18}$$

u_a^{ij} determines the destination of the drone that has delivered to $D_{a,h_{a,ij}}^{ij}$. For example, if $u_a^{ij} = 0$, the drone returns to T_a^i. If $u_a^{ij} = 1$, the drone flies toward T_{a+1}^i.

Figure 5 shows an example of the drone flight routes between T_a^i and T_{a+1}^i.

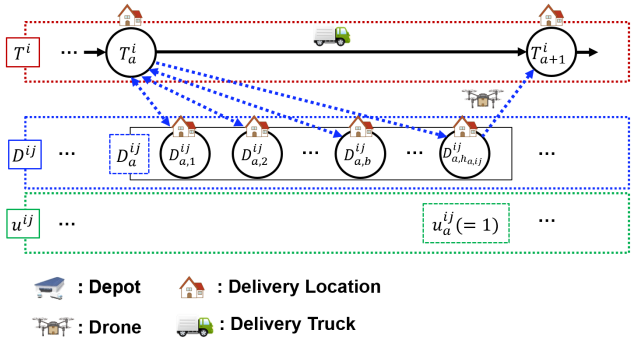

Fig. 5. One example of drone flight routes between T_a^i and T_{a+1}^i.

The following three types of mutation operators, as well as operators 1 to 5, are used to generate a hybrid delivery route. It should be noted that $c1$, $n1$, and $n2$ are arbitrary integers in the domain shown in Eqs. (19) and (20).

$$1 \le c1 \le h_{a,ij} \tag{19}$$

$$1 \le n1 \le n2 \le NH_i \tag{20}$$

Operator 6 :
T_{n1}^{a1} is selected from T^{a1} and D_{n2}^{a2b1} is selected from D^{a2b1}. Then T_{n1}^{a1} is inserted into an arbitrary place of D_{n2}^{a2b1}.

Operator 7 :
$D_{n1,c1}^{a1b1}$ is selected from D_{n1}^{a1b1} and inserted into an arbitrary place between two WPs of T^{a2}.

Operator 8 :
u_{n1}^{a1b1} is selected from u^{a1b1}. If $u_{n1}^{a1b1} = 1$, it is changed to $u_{n1}^{a1b1} = 0$. If $u_{n1}^{a1b1} = 0$, it is changed to $u_{n1}^{a1b1} = 1$.

4. Problem Setting

4.1. Delivery area

It is necessary to obtain map data related to the delivery area in advance in order to generate a delivery route. The Itoshima Peninsula in Japan was set as the delivery area for this study. The map image was obtained from Google Maps. The shape of the road was extracted from the quoted map, and one depot and 30 delivery positions were arranged on the road as shown in Fig. 6.

We assumed that the truck can travel on this road and the drone can travel in all areas except for over the mountains.

4.2. Pre-calculations

The solution search in the DDP can be made more efficient by referring to the shortest distance between the WPs that is calculated in advance when evaluating the generated delivery route. The shortest route is calculated for both the cases of land and air routes.

4.2.1. Land routes

We set points that can be reached by a truck on the road

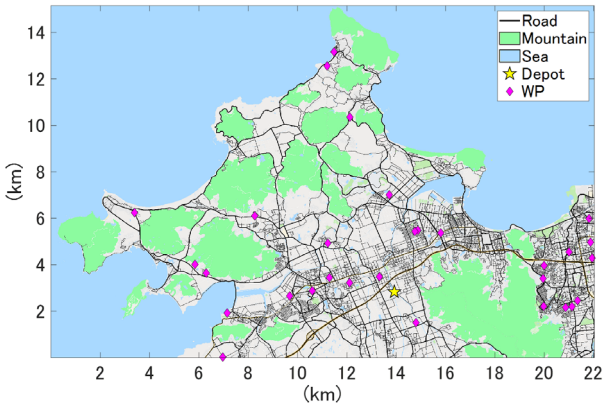

Fig. 6. Delivery area map.

as shown in Fig. 6. The interval between the points is within a range in where the road shape can be expressed by connecting them. The presence or absence of obstacles between the points can be determined using the ray-tracing method.[19] The shortest distance cost between WPs can be calculated using the distance cost between the points, the presence or absence of obstacles, and the A* algorithm.[20] Equation (21) represents one of the calculated shortest distance cost,

$$TC_{\boldsymbol{d1d2}} = TC_{\boldsymbol{d2d1}}, \quad (\boldsymbol{0} \le \boldsymbol{d1}, \boldsymbol{d2} \le \boldsymbol{N_{WP}}) \tag{21}$$

where, $\boldsymbol{d1}$ and $\boldsymbol{d2}$ are unique numbers used for discriminating each WP, $\boldsymbol{0}$ is a depot, and the values $\boldsymbol{1}$ through $\boldsymbol{N_{WP}}$ represent each delivery position. All of the shortest distance costs between WPs can be expressed as shown in Eq. (22).

$$TC = \begin{bmatrix} 0 & TC_{\boldsymbol{01}} & \cdots & TC_{\boldsymbol{0N_{WP}}} \\ TC_{\boldsymbol{10}} & 0 & & TC_{\boldsymbol{1N_{WP}}} \\ \vdots & & \ddots & \vdots \\ TC_{\boldsymbol{N_{WP}0}} & TC_{\boldsymbol{N_{WP}1}} & \cdots & 0 \end{bmatrix} \tag{22}$$

4.2.2. Flight routes

We set points that can be traveled by a drone on the map shown in Fig. 6, except for those in mountainous. The points are set at 4[m] vertical and horizontal intervals. The shortest flight distance between the WPs can be calculated in the same manner as that presented in Section 4.2.1. The flight distance costs between WPs were calculated and expressed as shown in Eq. (23).

$$DC_{\boldsymbol{d1d2}} = DC_{\boldsymbol{d2d1}} \tag{23}$$

All of the shortest flight distance costs between WPs are expressed as shown in Eq. (24).

$$DC = \begin{bmatrix} 0 & DC_{\boldsymbol{01}} & \cdots & DC_{\boldsymbol{0N_{WP}}} \\ DC_{\boldsymbol{10}} & 0 & & DC_{\boldsymbol{1N_{WP}}} \\ \vdots & & \ddots & \vdots \\ DC_{\boldsymbol{N_{WP}0}} & DC_{\boldsymbol{N_{WP}1}} & \cdots & 0 \end{bmatrix} \tag{24}$$

4.3. Formulation of the delivery route problems

The delivery route problems related to the truck, drone and hybrid deliveries are formulated as a constrained multi-objective optimization problem, as shown below.

4.3.1. Truck delivery

The truck delivery problem is formulated as follows.

$$\min_{\boldsymbol{x}} \boldsymbol{F}(\boldsymbol{x}) = \min_{\boldsymbol{x}} [F_1(\boldsymbol{x}), F_2(\boldsymbol{x}), F_3(\boldsymbol{x})]^T \tag{25}$$

$$F_1(\boldsymbol{x}) = \sum_{i=1}^{A} \sum_{a=0}^{NT_i} TC_{T_a^i T_{a+1}^i} \quad (\boldsymbol{T_0^i} = \boldsymbol{T_{NT_i+1}^i} = \boldsymbol{L_d} = \boldsymbol{0}) \tag{26}$$

$$F_2(\boldsymbol{x}) = \sum_{i=1}^{A}\left(\sum_{a=0}^{NT_i}\frac{TC_{\boldsymbol{T_a^i T_{a+1}^i}}}{V_T} + NT_i\left(t_p + t_{st} + t_{sp}\right)\right) \quad (27)$$

$$F_3(\boldsymbol{x}) = \sum_{i=1}^{A} T_{i,Count} \quad T_{i,Count} = \begin{cases} 1, & NT_i > 0 \\ 0, & NT_i = 0 \end{cases} \quad (28)$$

Subject to

$$g_1(\boldsymbol{x}) = F_1(\boldsymbol{x}) \le LD_{max} \quad (29)$$
$$g_2(\boldsymbol{x}) = F_2(\boldsymbol{x}) \le LT_{max} \quad (30)$$
$$g_3(\boldsymbol{x}) = F_3(\boldsymbol{x}) = A \quad (31)$$

Where, Eqs. (26) through (28) present the total delivery distance, total delivery time required to complete the delivery service, and number of trucks used, respectively. Equations (29) through (31) are the constrained conditions of $F_1(\boldsymbol{x})$ through $F_3(\boldsymbol{x})$, respectively.

4.3.2. Drone delivery

The drone delivery problem is formulated as follows.

$$\min_{\boldsymbol{x}} \boldsymbol{F}(\boldsymbol{x}) = \min_{\boldsymbol{x}} [F_4(\boldsymbol{x}), F_5(\boldsymbol{x}), F_6(\boldsymbol{x})]^T \quad (32)$$

$$F_4(\boldsymbol{x}) = 2\sum_{j=1}^{B}\sum_{b=1}^{ND_i} DC_{\boldsymbol{L_d D_b^j}} \quad (33)$$

$$F_5(\boldsymbol{x}) = \sum_{j=1}^{B}\left(\sum_{b=1}^{ND_i}\frac{2DC_{\boldsymbol{L_d D_b^j}}}{V_D} + ND_i \times (t_{re} + 4t_{tl})\right) \quad (34)$$

$$F_6(\boldsymbol{x}) = \sum_{j=1}^{B} D_{j,Count} \quad D_{j,Count} = \begin{cases} 1, & ND_i > 0 \\ 0, & ND_i = 0 \end{cases} \quad (35)$$

Subject to

$$g_1(\boldsymbol{x}) = F_6(\boldsymbol{x}) = B \quad (36)$$
$$g_2(\boldsymbol{x}) = \frac{2DC_{\boldsymbol{L_d D_b^j}}}{V_D} + 4t_{tl} \le t_d \quad (37)$$
$$g_3(\boldsymbol{x}) = w_b^j \le W_d \quad (38)$$

Where, Eqs. (33) through (35) present the total flight delivery distance, total flight time, and number of drones used, respectively. Equation (36) is the constrained conditions of $F_6(\boldsymbol{x})$. Equations (37) and (38) present the constrained conditions related to the flight duration and loadable weight of the drone, respectively.

4.3.3. Hybrid delivery

The hybrid delivery problem is formulated as follows.

$$\min_{\boldsymbol{x}} \boldsymbol{F}(\boldsymbol{x}) = \min_{\boldsymbol{x}} [F_1(\boldsymbol{x}), F_2(\boldsymbol{x}), \dots, F_6(\boldsymbol{x})]^T \quad (39)$$

$$F_1(\boldsymbol{x}) = \textstyle\sum_{i=1}^{A}\sum_{a=0}^{NH_i} TC_{\boldsymbol{T_a^i T_{a+1}^i}} \quad \left(\boldsymbol{T_0^i = T_{NH_i+1}^i = L_d = 0}\right) \quad (40)$$

$$F_2(\boldsymbol{x}) = \sum_{i=1}^{A}\sum_{a=0}^{NH_i}\left(f_{1,ai}(\boldsymbol{x}) + f_{3,ai}(\boldsymbol{x}) + u_a^{ij} \times t_{re}\right) \quad (41)$$

$$F_3(\boldsymbol{x}) = \sum_{i=1}^{A} T_{i,Count} \quad T_{i,Count} = \begin{cases} 1, & NH_i > 0 \\ 0, & NH_i = 0 \end{cases} \quad (42)$$

$$F_4(\boldsymbol{x}) = \textstyle\sum_{i=1}^{A}\sum_{j=1}^{B}\sum_{a=0}^{NH_i}\left(f_{1,aij}(\boldsymbol{x}) + f_{2,aij}(\boldsymbol{x}) + f_{3,aij}(\boldsymbol{x})\right) \quad (43)$$

$$F_5(\boldsymbol{x}) = \sum_{i=1}^{A}\sum_{j=1}^{B}\sum_{a=0}^{NH_i}\left(f_{6,aij}(\boldsymbol{x}) + f_{7,aij}(\boldsymbol{x})\right) \quad (44)$$

$$F_6(\boldsymbol{x}) = \sum_{i=1}^{A}\sum_{j=1}^{B} D_{ij,Count}, \; D_{ij,Count} = \begin{cases} 1, & \sum_{a=0}^{NH_i} h_{a,ij} > 0 \\ 0, & \sum_{a=0}^{NH_i} h_{a,ij} = 0 \end{cases} \quad (45)$$

Where,

$$f_{1,aij}(\boldsymbol{x}) = 2\sum_{b=1}^{h_{a,ij}-1} DC_{\boldsymbol{T_a^i D_{a,b}^{ij}}} \quad (46)$$

$$f_{2,aij}(\boldsymbol{x}) = (1 - u_a^{ij}) \times 2DC_{\boldsymbol{T_a^i D_{a,h_{a,ij}}^{ij}}} \quad (47)$$

$$f_{3,aij}(\boldsymbol{x}) = u_a^{ij} \times \left(DC_{\boldsymbol{T_a^i D_{a,h_{a,ij}}^{ij}}} + DC_{\boldsymbol{D_{a,h_{a,ij}}^{ij} T_{a+1}^i}}\right) \quad (48)$$

$$f_{4,aij}(\boldsymbol{x}) = \frac{f_{1,aij}(\boldsymbol{x})}{V_D} + 4t_{tl}\left(h_{a,ij} - 1\right) \quad (49)$$

$$f_{5,aij}(\boldsymbol{x}) = (1 - u_a^{ij}) \times \left(\frac{f_{2,aij}(\boldsymbol{x})}{V_D} + 4t_{tl}\right) \quad (50)$$

$$f_{6,aij}(\boldsymbol{x}) = u_a^{ij} \times \left(\frac{f_{3,aij}(\boldsymbol{x})}{V_D} + 4t_{tl}\right) \quad (51)$$

$$f_{7,aij}(\boldsymbol{x}) = f_{4,aij}(\boldsymbol{x}) + f_{5,aij}(\boldsymbol{x}) + t_{re}\left(h_{a,ij} - u_a^{ij}\right) \quad (52)$$

$$f_{1,ai}(\boldsymbol{x}) = max\left\{f_{7,ai1}(\boldsymbol{x}), f_{7,ai2}(\boldsymbol{x}), \dots, f_{7,aiB}(\boldsymbol{x})\right\} \quad (53)$$

$$f_{2,ai}(\boldsymbol{x}) = \frac{TC_{\boldsymbol{T_a^i T_{a+1}^i}}}{V_T} + t_p + t_{st} + t_{sp} \quad (54)$$

$$f_{3,ai}(\boldsymbol{x}) = max\left\{f_{2,ai}(\boldsymbol{x}), f_{6,ai1}(\boldsymbol{x}), f_{6,ai2}(\boldsymbol{x}), \dots, f_{6,aiB}(\boldsymbol{x})\right\} \quad (55)$$

Subject to

$$g_1(\boldsymbol{x}) = F_1(\boldsymbol{x}) \le LD_{max} \quad (56)$$
$$g_2(\boldsymbol{x}) = F_2(\boldsymbol{x}) \le LT_{max} \quad (57)$$
$$g_3(\boldsymbol{x}) = F_3(\boldsymbol{x}) = A \quad (58)$$
$$g_4(\boldsymbol{x}) = \frac{2DC_{\boldsymbol{T_a^i D_{a,b}^{ij}}}}{V_D} + 4t_{tl} \le t_d \quad (59)$$
$$g_5(\boldsymbol{x}) = \frac{f_{3,aij}(\boldsymbol{x})}{V_D} + 4t_{tl} \le t_d \quad (60)$$
$$g_6(\boldsymbol{x}) = F_6(\boldsymbol{x}) = B \quad (61)$$
$$g_7(\boldsymbol{x}) = w_{a,b}^{ij} \le W_d \quad (62)$$

Where, Eqs. (40) through (45) present the total delivery distance, total delivery time required to complete the delivery service, number of trucks used, total flight delivery distance, total flight time, and number of drones used, respectively. Equation (46) presents the total flight distance required to complete the delivery from $D_{a,1}^{ij}$ to $D_{a,h_{a,ij}-1}^{ij}$. Equation (47) presents the flight distance to complete the delivery at $D_{a,h_{a,ij}}^{ij}$ and return to T_a^i. Equation (48) presents the flight distance to complete the delivery at $D_{a,h_{a,ij}}^{ij}$ and move to T_{a+1}^i. Equations (49) through (51) represent the flight times of Eqs. (46) through (48), respectively. Equation (52) presents the time between when the truck arrives at T_a^i and when it starts to move to T_{a+1}^i. Equation (53) presents the auxiliary of Eq. (41). Equation (54) presents the time between when the truck leaves at T_a^i and when it completes the delivery T_{a+1}^i. Equation (55) presents the maximum value of Eqs. (51) and Eq. (54). Equations (56) through (58) and Eq. (61) present the constrained conditions of $F_1(\boldsymbol{x})$ through $F_3(\boldsymbol{x})$, and $F_6(\boldsymbol{x})$, respectively. Equations (59) and (60) are the constrained conditions related to the drone flight duration. Equation (62) presents the constrained conditions related to the drone loadable weight.

4.4. Conversion factors

All of the objective functions presented in Section 4.3 are now converted into delivery costs. According to the 2017 business analysis report released by the Japan Truck Association, the delivery costs of the service are divided into four categories: labor cost, fuel cost, maintenance cost, and depreciation cost.[21] Figure 7 shows the percentage of each

category.

Assuming that the evaluation values of the truck delivery route correspond to the percentages in Fig. 7, the following equations are obtained.

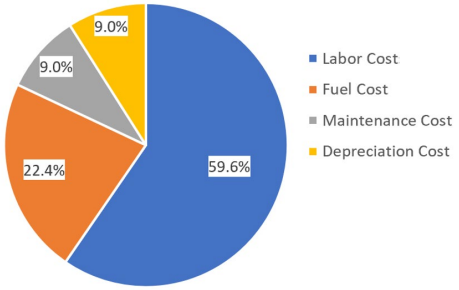

Fig. 7. Breakdown of the delivery costs.

$$\frac{CF_2 \times F_2(x)}{CF_1 \times F_1(x) + CF_2 \times F_2(x) + CF_3 \times F_3(x)} = 0.596 \quad (63)$$

$$\frac{CF_1 \times F_1(x)}{CF_1 \times F_1(x) + CF_2 \times F_2(x) + CF_3 \times F_3(x)} = 0.314 \quad (64)$$

$$\frac{CF_3 \times F_3(x)}{CF_1 \times F_1(x) + CF_2 \times F_2(x) + CF_3 \times F_3(x)} = 0.09 \quad (65)$$

Where, CF_1, CF_2, and CF_3 are calculated from the above equations. It is also assumed that the drone's conversion factors are determined based on the relative cost ratio of the drone to that of the truck. In this case, CF_4, CF_5, and CF_6 are calculated using the following equations.

$$CF_4 = R \times CF_1 \quad (66)$$

$$CF_5 = R \times CF_2 \quad (67)$$

$$CF_6 = R \times CF_3 \quad (68)$$

5. Calculation Results

5.1. Verification of the improved PIP method

We verified the usefulness of the improved PIP method using the TSPLIB and the DDP. Note that the TSPLIB is a single-objective optimization problem where the objective function is only the distance of the generated path, and no constraints are given. Therefore, the benchmark tests in this section evaluate only the improvement in solution search performance by combining the TS and original PIP method.

5.1.1. TSPLIB

We compared the solution search performance of the improved PIP method to that form the original PIP method using some benchmark problems of the TSPLIB; specifically, "berlin52," "eli76," "lin105," "ch150," and "KroA200."[18] The solution structure and mutation operators are the same as those presented in Section 3.1. As a selection operation, we applied the strategy of inheriting only the upper individual to the next generation, $E_n = 20$ is set for the original PIP method, and $E_n = 1$ is set for the improved PIP method. The solution search ends at $G_{max} = 500{,}000$. We also set $P_n = 200$, $G_{tabu} = 1000$, and the number of each calculation sample as 10. The calculation software was MATLAB ver. 2018b, and the CPU of the PC used was an Intel Core i7-4790 3.60 GHz CPU with 8 GB of RAM.

Figure 8 shows a comparison of two error ratio graphs showing the distance cost for the generated route and shortest route. From this result, it can be observed that the error rates and standard deviations of the improved PIP method are smaller than those of the original PIP method.

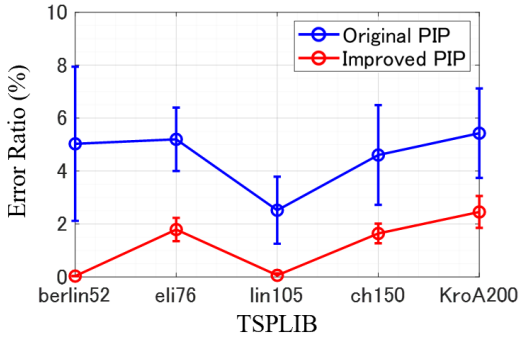

Fig. 8. Comparison of the search performance.

Furthermore, we applied the original PIP method and the improved PIP method to "eli76" under the five calculation conditions shown in Table 1, respectively, and compared the error ratio and calculation time of the generated solution and the optimal value.

Table 1. Calculation conditions of G_{max} and G_{tabu} for each case.

Case	G_{max}	G_{tabu}
Case 1	10,000	10
Case 2	50,000	50
Case 3	100,000	100
Case 4	150,000	150
Case 5	200,000	200

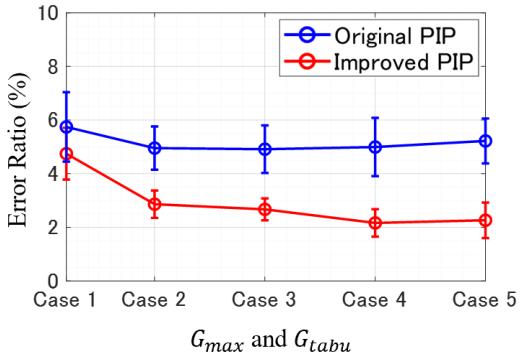

Fig. 9. Comparison of the search performance for each case.

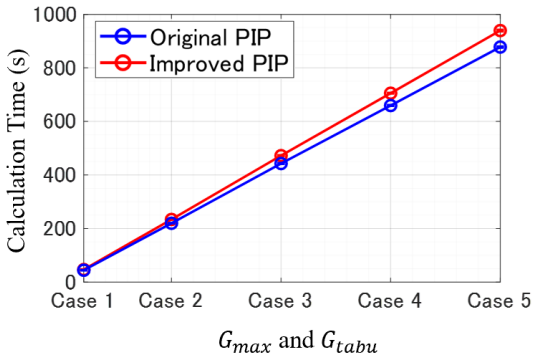

Fig. 10. Comparison of the calculation times for each case.

Figure 9 shows that the improvement effect of the error ratio in the improved PIP method by increasing G_{max} and G_{tabu} is larger than that of the original PIP method. The reason for this is that the IC problem can be avoided by the TS, and convergence of the solution search is improved by increasing G_{max} and G_{tabu}.

Figure 10 shows that the calculation time of the improved PIP method is longer than that of the original PIP method. This is because it is necessary to remove the solution included in TL from the population. The reason why the difference in calculation time increases as the values of G_{max} and G_{tabu} increase is the number of solutions in the TL increases as the number of generations increases.

From the above results, we found that the solution search performance of the improved PIP method improves as G_{max} and G_{tabu} increase, unlike the original PIP method. However, it is necessary to set G_{max} and G_{tabu} appropriately because the rate of increase in calculation time for the improved PIP method is larger than that of the original PIP method.

5.1.2. DDP

In order to verify the usefulness of the improved PIP method, we compared it with the original PIP method in terms of the probability of successfully generating a feasible solution and the total delivery cost of the obtained delivery route. The calculation conditions are listed in Table 2.

In addition, we calculated the shortest truck delivery route in Fig. 6 using the GA in order to obtain the values of CF_1 to CF_6 using Eqs. (63) to (68), respectively. Figure 11 shows the generated delivery route. The number attached to each WP in this figure represents the delivery order. As a result, $F_1(\boldsymbol{x}) = 81{,}229$ [m], $F_2(\boldsymbol{x}) = 12{,}463$ [s], and $F_3(\boldsymbol{x}) = 1$ [truck]. Then, we can obtain $CF_1 = 0.0213$ [yen/m], $CF_2 = 0.264$ [yen/s], $CF_3 = 497$ [yen/truck], $CF_4 = 0.00213$ [yen/m], $CF_5 = 0.0264$ [yen/s], and $CF_6 = 49.7$ [yen/drone].

Table 2. Calculation conditions.

Items	Values	Unit	Items	Values	Unit
P_n	100	Individuals	t_d	30	min
G_{tabu}	10	Generations	t_{tl}	30	s
G_{max}	5000	Generations	t_{re}	30	s
A	1	Trucks	t_p	2	min
B	1	Drones	W_d	2	kg
N_{WP}	30	Places	$w_{a,b}^{ij}$	1-2	kg
V_t	10	m/s	LD_{max}	50,000	m
V_d	15	m/s	LT_{max}	10,000	s
R	0.1				

We first compare the success rates of generating a feasible solution in Procedure 1. The number of calculation samples is 100. It should be noted that $E_n = 10$ is set for the original PIP method, and $E_n = 1$ is set for the improved PIP method. Figure 12 presents the result of the comparison of the solution searches.

From this figure, the success rate of generating a feasible solution using the improved PIP method is 100%, but that of the original PIP method is only 36%.

Next, the delivery cost of the obtained delivery route using

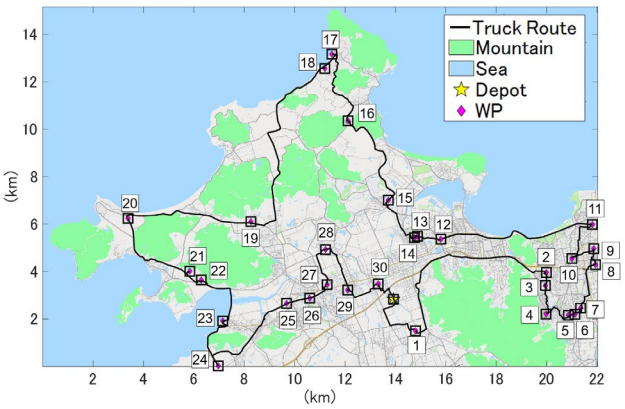

Fig. 11. Generated truck delivery route.

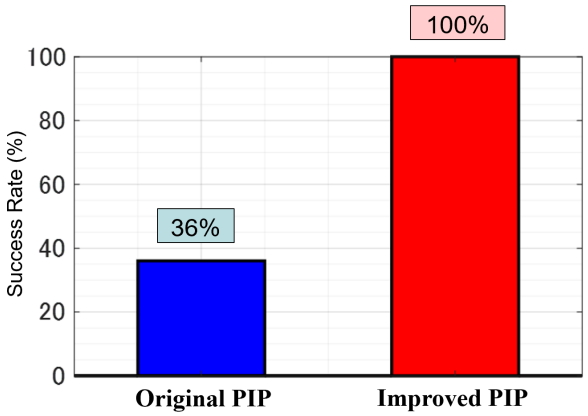

Fig. 12. Comparison of the success rates of generating a feasible solution.

Procedure 2 is compared. Some of the given constrained conditions were relaxed to $LD_{max} = 100{,}000$ [m] and $LT_{max} = 14{,}400$ [s], such that feasible solutions can be generated regardless of the method used.

Figure 13 shows the average delivery costs and the standard deviations of the hybrid delivery routes generated using the original and improved PIP methods, respectively. As per this result, the delivery routes generated using the improved PIP method have lower costs of approximately 6.2% on average when compared to those of the original PIP method. The standard deviation of the improved PIP method was suppressed to approximately half that of the original PIP method. Therefore, the solution search performance of the improved PIP method is superior to that of the original PIP method.

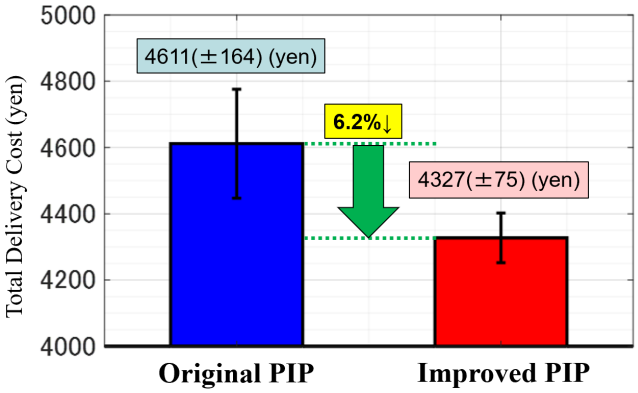

Fig. 13. Comparison of the total delivery cost.

5.2. Relationship between cost-reduction effect and R

We calculated the delivery cost-reduction rate in the range of $0 \leq R \leq 1$ in order to analyze the relationship between R and the cost-reduction effect of the drone delivery service. In order to obtain feasible solutions in all of the delivery styles, the constraint condition was relaxed to $LD_{max} = 100{,}000$ [m], and $LT_{max} = 30{,}000$ [s]. The other conditions are the same as those listed in Table 2.

Figure 14(a) shows the generated drone delivery route. The number attached to each WP in the figure represents the delivery order. The evaluation values of the objective functions are $F_4(\boldsymbol{x}) = 381{,}592$ [m], $F_5(\boldsymbol{x}) = 29{,}039$ [s], and $F_6(\boldsymbol{x}) = 1$ [drone].

Figure 14(b) shows the hybrid delivery route, which is generated by combining a truck and drone, as shown in Fig. 1 (c). The number attached to each WP in this figure represents the delivery order. The evaluation values of the objective functions are $F_1(\boldsymbol{x}) = 52{,}947$ [m], $F_2(\boldsymbol{x}) = 8{,}416$ [s], $F_3(\boldsymbol{x}) = 1$ [truck], $F_4(\boldsymbol{x}) = 76{,}623$ [m], $F_5(\boldsymbol{x}) = 6{,}908$ [s], and $F_6(\boldsymbol{x}) = 1$ [drone].

Figure 15 presents the graphs showing how much the average delivery cost can be reduced by using the drone delivery route and the hybrid delivery route as compared to the truck delivery route for the range of $0 \leq R \leq 1$. The standard deviations are displayed at each plot point. The number of samples at these points is 10.

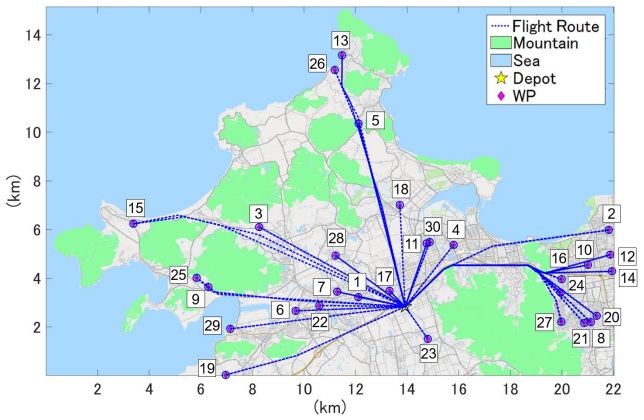

Fig. 14(a). Generated drone delivery route.

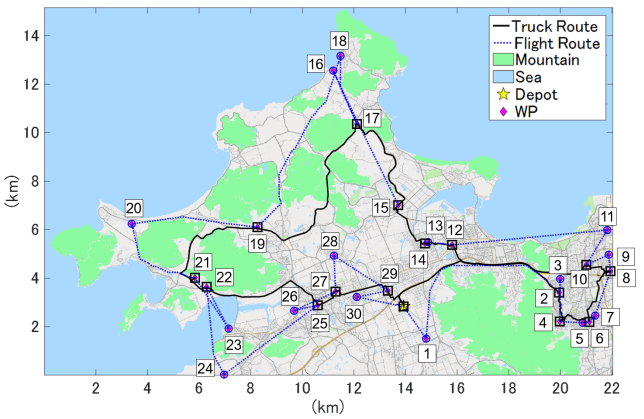

Fig. 14(b). Generated hybrid delivery route.

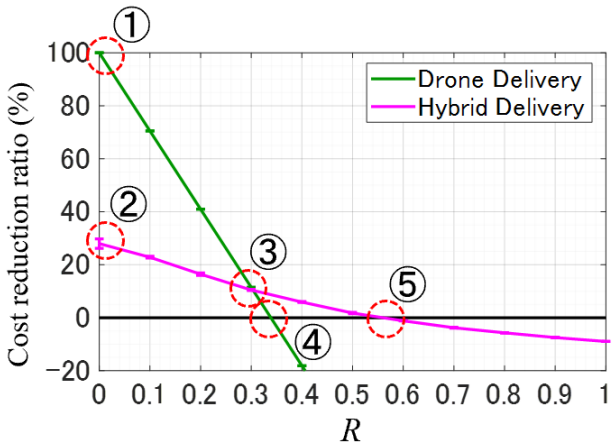

Fig. 15. Cost-reduction ratio graph of the drone delivery and hybrid delivery as compared to that of the truck delivery.

The following facts can be stated regarding points ① through ⑤, as indicated by the red broken line in the figure above.

① When $R = 0$, the cost-reduction ratio of the drone delivery is 100%.

② When $R = 0$, the cost-reduction ratio of the hybrid delivery is less than 30%.

③ When $R = 0.3$, the cost-reduction ratios of the drone and hybrid deliveries are nearly the same.

④ When $R > 0.3$, the cost-reduction effect of the drone delivery is lost.

⑤ When $R > 0.5$, the cost-reduction effect of the hybrid delivery is lost.

Based on the above facts, the following knowledge regarding the cost-reduction effect of the drone delivery service was determined.

- The smaller the value of R, the greater the cost-reduction effect.
- Drone delivery has a greater cost-reduction effect than that of the hybrid delivery owing to the increase in the value of R.
- Whether drone or hybrid delivery is superior in terms of the cost-reduction effect depends on the value of R.

The above knowledges obtained is valid under the assumptions we made, and will change depending on the values of conversion factors. However, the conversion factors are set reflecting the current statistics, and knowledge gained has some important meanings for the current cost ratios of relevant factors. It is meaningful to examine the effects of change in the conversion factors on cost-reduction as future work.

6. Conclusion

In this paper, we presented an improved PIP method that prevents the occurrence of the DBZ problem and IC problems that occur when the original PIP method is applied to the DDP. The proposed method prevents occurrence of the DBZ problem by transforming the DDP into a single-objective optimization problem of delivery cost using conversion factors. Furthermore,

it can also handle the IC problem by combining TS with the original PIP method.

We evaluated the validity of the proposed method using some types of benchmark problems from the TSPLIB and DDP. As a result, we found that the improved PIP method can generate the shortest paths that are closer to the optimal solution than those obtained using the original PIP method. However, appropriate parameter settings are required in order to perform an efficient solution search of the improved PIP method. We also found that the improved PIP method is superior in terms of the success rate for generating a feasible solution and reducing the delivery cost as compared to those of the original PIP method.

Finally, we analyzed the relationship between the cost-reduction effect of the drone delivery service and the relative cost ratio of the drone to the truck using the improved PIP method. As a result, we obtained significant knowledges regarding the cost-reduction effect of drone delivery services.

References

1) Besada, J., Bergesio, L., Campaña, I., Vaquero-Melchor, D., López-Araquistain, J., Bernardos, A., and Casar, J.: Drone Mission Definition and Implementation for Automated Infrastructure Inspection Using Airborne Sensors, *Sensors*, **18**(2018), p. 1170.
2) Kaleem, Z. and Rehmani, M. H.: Amateur Drone Monitoring: State-of-the-Art Architectures, Key Enabling Technologies and Future Research Directions, *Wirel. Commun., IEEE J.*, **25**(2018), pp. 150–159.
3) Mogili, U. R. and Deepak, B. B. V. L.: Review on Application of Drone Systems in Precision Agriculture, *Proc. Comp. Sci.*, **133**(2018), pp. 502–509.
4) Harvey, M. C., Rowland, J. V., and Luketina, K. M.: Drone with Thermal Infrared Camera Provides High Resolution Georeferenced Imagery of the Waikite Geothermal Area, *New Zealand. J. Volcan. Geotherm. Res.*, **325**(2016), pp. 61–69.
5) Claesson, A., Bäckman, A., Ringh, M., Svensson, L., Nordberg, P., Djärv, T., and Hollenberg, J.: Time to Delivery of an Automated External Defibrillator Using a Drone for Simulated Out-of-Hospital Cardiac Arrests vs Emergency Medical Services, *JAMA*, **317**(2017), pp. 2332–2334.
6) Wilson, R. L.: Ethical Issues with Use of Drone Aircraft, *In Proceedings of the IEEE 2014 International Symposium on Ethics in Engineering, Science, and Technology.*, IEEE Press 2014–5, 2014.
7) Dorling, K., Heinrichs, J., Messier, G. G., and Magierowski, S.: Vehicle Routing Problems for Drone Delivery, *Trans. Syst., Man, Cyber.: Syst., IEEE J.*, **47**(2016), pp. 70–85.
8) Muramatsu, N. and Akiyama, H.: Super-Aging Society Preparing for the Future, *Gerontol*, **51**(2011), pp. 425–432.
9) Boysen, N., Schwerdfeger, S., and Weidinger, F.: Scheduling Last-Mile Deliveries with Truck-Based Autonomous Robots, *Europ. J Operat. Res.*, **271**(2018), pp. 1085–1099.
10) Rabta, B., Wankmüller, C., and Reiner, G.: A Drone Fleet Model for Last-Mile Distribution in Disaster Relief Operations, *Int. J. Disaster Risk Reduct.*, **28**(2018), pp. 107–112.
11) Murray, C. C. and Chu, A. G.: The Flying Sidekick Traveling Salesman Problem: Optimization of Drone-Assisted Parcel Delivery, *Transport. Res. Part C: Emerg. Technol.*, 54(2015), pp. 86–109.
12) Ferrandez, S. M., Harbison, T., Weber, T., Sturges, R., and Rich, R.: Optimization of a Truck-Drone in Tandem Delivery Network Using k-Means and Genetic Algorithm, *J. Indust. Eng. Manag. (JIEM)*, **9**(2016), pp. 374–388.
13) Omagari, H. and Higashino, S. I.: Provisional-Ideal-Point-Based Multi-Objective Optimization Method for Drone Delivery Problem, *Int. J. Aeronaut. Space Sci.*, **19**(2018), pp. 262–277.
14) Omagari, H.: Potential Benefits Assessment on Home Delivery Service Using Multiple Drones. *In Proceedings of the 31st International Council of Aeronautical Sciences*, Belo Horizonte, Brazil, ICAS 2018-9, 2018.
15) Chiang, W. C., Li, Y., Shang, J., and Urban, T. L.: Impact of Drone Delivery on Sustainability and Cost: Realizing the UAV Potential Through Vehicle Routing Optimization, *J. Appl. Energ.*, **242**(2019), pp. 1164–1175.
16) Goodchild, A. and Toy, J.: Delivery by Drone: An Evaluation of Unmanned Aerial Vehicle Technology in Reducing CO2 Emissions in the Delivery Service Industry, *Transport. Res. Part D: Transport Environ.*, 61(2018), pp. 58–67.
17) Gendreau, M., Hertz, A., and Laporte, G.: A Tabu Search Heuristic for the Vehicle Routing Problem. *Manag. Sci.,* **40**(1994), pp. 1276–1290.
18) Reinelt, G.: TSPLIB—A Traveling Salesman Problem Library, *ORSA J. Comput.*, **3**(1991), pp. 376–384.
19) Amanatides, J. and Woo, A.: A Fast Voxel Traversal Algorithm for Ray Tracing. *Eurograph* **87**(1987), pp. 3–10.
20) Mitsutake, K. and Higashino, S.: An A*-EC Hybrid Path Planning Method for Waypoints Traveling Problem Considering Terrain, AIAA Guid., Navig. Contr. Conf. Exhibit, 2008.
21) Japan Trucking Association, *Current Status and Issues of the Truck Transportation Industry in Japan*, JTA Publishing, Tokyo, 2019, p. 14 (in Japanese).